Desalination and Water Treatment
www.deswater.com

doi: 10.1080/19443994.2016.1140086

57 (2016) 24187–24199
November

Taylor & Francis
Taylor & Francis Group

Characteristic of single/mixed organic foulants on nanofiltration membrane and prompt fouling predictor method

Fang Gao[a,b,c], Yuxing Sheng[a,b,*], Yuping Li[a,b], Hongbin Cao[a,b], Haibo Li[a,b]

[a]*National Engineering Laboratory for Hydrometallurgical Cleaner Production Technology, Institute of Process Engineering, Chinese Academy of Sciences, Beijing 100190, P.R. China, Tel./Fax: +86 10 82544844; emails: 232230204@qq.com (F. Gao), yxsheng@home.ipe.ac.cn (Y. Sheng), stringsplay@126.com (Y. Li), Tel./Fax: +86 10 82544839; email: hbcao@home.ipe.ac.cn (H. Cao), Tel./Fax: +86 10 82544844; email: hbli@home.ipe.ac.cn (H. Li)*

[b]*Key Laboratory of Green Process and Engineering, Institute of Process Engineering, Chinese Academy of Sciences, Beijing 100190, P.R. China*

[c]*University of Chinese Academy of Sciences, Beijing 100049, P.R. China*

Received 9 November 2015; Accepted 2 January 2016

ABSTRACT

The fouling behavior of nanofiltration (NF) membranes by proteins bovine serum album (BSA), lysozyme (LYS), and humic acids (HA), as well as their mixtures was studied in a cross flow bench-scale cell. The similarities and differences of the effects of pH on single and mixed organic foulant systems were compared by analyzing the size distribution and zeta potential of foulants in the feed, and in conjunction with the characterization of fouled NF membranes, respectively. Results showed that the fouling behaviors of both single and the mixed systems were significantly correlative with solution pH, moreover BSA/LYS combined with HA appeared more aggravated fouling behavior than single foulant within the test pH range. For solution pH, this can affect interactions of foulants–foulants and foulants–membrane by changing zeta potential of them. Also, therefore, zeta potential value could be used to predict the fouling behavior of NF. Considering the experimental results, more severe fouling behavior by not only single (HA, BSA, and LYS), but mixed systems (BSA + HA and LYS + HA) occurred at acidic and neutral solution pH.

Keywords: Nanofiltration; Organic foulant; Zeta potential; Fouling mechanism

1. Introduction

Nanofiltration (NF) as an effective purification and separation technology is widely and increasingly used to produce pure water and separation multivalent dissolve inorganic salt from brackish water or wastewater [1–6]. NF membrane fouling, which may decrease water production and desalination during filtration and increase operating costs caused by frequent plant shutdowns for in situ membrane cleaning, is a problem that requires immediate attention [7,8].

NF membrane fouling involves inorganic salt fouling or scaling, natural organic matter (NOM) fouling, biofouling, and fouling by colloidal particle [9–12]. NOM, such as organic acids and proteins in water and wastewater, is identified as the major factor in dominating NF membrane fouling. Moreover, a number of studies about the fouling behavior and mechanism of organic foulants on the membrane are

*Corresponding author.

available, and the consensus among these reports have shown that fouling aggravation occurs with the formation of the fouling gel/cake on the membrane [13–15]. Contreras et al. [16] have investigated the effect of functional groups of single protein on foulant absorption and fouling cake formation on NF and reverse osmosis membrane. In addition, NF membranes' surface with different charge is also related to organic fouling behavior. Their studies emphasized that electrostatic force between the foulant and membrane surface functional groups has a domination role on fouling potential [17–19]. Existing literatures illustrated that the zeta potential of the organic foulants as characterization of electrostatic force can be influenced by solution pH [20,21]. For example, Jones et al. [22] investigated the effect of solution pH on single humic acids (HA) foulant, and the results indicated that the decreasing of solution pH can weaken the zeta potential of HA and lead to increasing fouling rate, which was attributed to the lack of electrostatic repulsion between the molecules. Additionally, the fouling behavior of single bovine serum albumin (BSA) protein on the microfiltration (MF) and ultrafiltration membranes has also been studied, and their conclusions indicate that the most severe fouling behavior occurs near the isoelectric point (IEP) of BSA [23].

In real wastewater, the typical feed solution for NF membrane usually contains different foulants, and the fouling mechanisms are more complex due to not just the interaction between foulants and membrane, but also the interaction between variant foulants. Relatively, few studies have reported interactions between different organic foulants with respect to influence of zeta potential. Palacio et al. [24] studied that effect of mixed BSA and lysozyme (LYS) composition on MF fouling showed that mixtures with amounts of BSA decreasing fouled more slowly than observed with either of the pure proteins, which may be attributed to electrostatic interactions between the BSA and LYS. On the contrary, a majority of investigations on fouling by mixed foulants addressed that the fouling by the mixture of BSA and alginate revealed more severe compared to that induced by BSA and alginate alone [25,26]. Wang et al. [27,28], in a study of the zeta potential of two types of proteins, describe that experienced more severe flux decline by the mixed proteins occurred within the IEPs of the two proteins. Therefore, characterization of such organic inter-foulant-compound interactions, including the zeta potential value of single/mixed organic foulant is important for understanding of membrane fouling mechanisms and anticipating the fouling degree on NF membrane.

This study aims to investigate the regular zeta potential of foulants that affect the single- or mixed-fouling system of NF membrane. HA and proteins are identified as the major organic matters in water and wastewater and considered to be widespread in membrane fouling, as well as their mixed foulants. The BSA and LYS are used as oppositely charged macromolecules, whereas HA is used as an example of smaller organic molecule comparing with the proteins. This study also aims to identify the similarities and differences of the effect of zeta potential on single- and mixed-fouling mechanisms by comparing the permeate flux loss of the fouled NF membranes, characterizing the aggregation and zeta potential of foulants by dynamic light scattering (DLS), and characterizing the virgin and fouled membranes by atomic force microscopy (AFM) and Fourier Transform infrared spectroscopy (FT-IR). The zeta potential values of the foulants are used as the indices of the fouling behavior of NF membrane and degree at constant operation pressure.

2. Materials and methods

2.1. Model organic foulants

HA (Sigma-Aldrich 53,680) was dissolved into ultrapure water as stock solutions (1 g L^{-1}) adjusted to pH 9.05 with NaOH, given the low acidic property of HA. Each HA foulant solution was prepared by diluting the required amount of foulant solution to experimental mass concentration. BSA (Sigma–Aldrich A1933, ≥98% purity) and LYS (Sigma–Aldrich L6876, ≥90% purity) were used as model protein foulants and stored at 4˚C in the dark. All reagents and chemicals were of analytical grade with purity over 99%, unless otherwise specified. Ultrapure water (Milli-Q, resistivity of 18.2 MΩ) was used to prepare the working solutions.

2.2. NF membrane

The membrane investigated in this study was a highly antifouling, thin-film composite NF (GL by GE Osmonics, Inc., US). The test membranes were placed in ultrapure water, which was replaced every week. The membrane had a molecular weight cut-off of 150–300 Da, and the rejection of 2,000 mg L^{-1} $MgSO_4$ was above 96% at the operation pressure of 110 psi. The contact angle of the GL membrane was 30.1˚. The GL membrane had a smooth surface with average roughness (R_a) = ~13.4 nm and root-mean-square roughness (R_q) = ~16.2 nm.

2.3. Membrane filtration test

NF experiments were performed in a laboratory scale cross-flow membrane filtration system that

consists of a membrane cell made of 316 L stainless steel with an active membrane area of 19.6 cm^2. A gear pump that adjusts the cross-flow velocity (WT3000-1JB-A; Longer Pump, China) was used to transport the feed solution. The applied pressure and cross-flow velocity inside the test cell were adjusted using a needle valve and monitored using a pressure transmitter (0–25 bar; SSI Technologies, Inc., China). Permeate flux was measured with an electronic balance (Ohaus Instruments Co., Ltd, China), and the obtained data were recorded by a computer data logging system. During filtration, the permeation and retention were recycled back to the feed tank at predetermined periods to avoid the influence of the concentration variation of organic pollutants on the osmotic pressure in the feed.

For each filtration, the new membrane was placed in ultrapure water until loaded into the test cell. The new membrane was initially compacted in pure water for 2 h to ensure the stability of permeate flux before the fouling test. For all experiments, the applied pressure was set at 70 psi and the cross-flow velocity at 0.08 m s^{-1}. Model organic foulant solutions consisted of dissolved HA, BSA, or LYS alone and equal amounts of dissolved BSA + or LYS + HA mixed system (i.e. the mass ratio of BSA and HA at 1:1 w/w). And total ionic strength of all feed solution was 10 mM adjusted by NaCl. The zeta potential values of single and mixed systems were adjusted by changing the pH using NaOH or HCl solution. Filtration tests that only contained single or mixed organic fouling system were continued for approximately 30 h to obtain the desired decline in the amount of flux at the end of the test.

2.4. Determination of foulant zeta potential

The zeta potential of single foulant (HA, BSA, and LYS) or mixed foulants (BSA + HA and LYS + HA) in the feed solution was measured using a Zetasize Nano-ZS (Beckman Coulter, Inc., USA). All model fouling systems were used in the measurements prior to the filtration experiments, and each condition was measured in at least two replicates.

2.5. Attenuated total reflection-Fourier Transform infrared spectroscopy

Attenuated total reflection-Fourier Transform infrared spectroscopy (ATR-FT-IR) was employed to identify the functional groups on the virgin and fouled NF membrane surfaces and to analyze the composition of the potential foulants. ATR-FT-IR used T27-Hyperion-Vector 22 (Bruker, Germany), and scans were performed at a wavelength of 4,000 and 500 cm^{-1}. Prior to ATR-FT-IR analysis, all membrane samples were dried in a desiccator to prevent interference by feed solution.

2.6. Atomic force microscopy measurements

AFM (Bruker Multimode 8, Germany) was used to measure the roughness of the virgin and fouled NF membranes, as well as compare and identify the tendency of different fouled NF membranes according to tests. All testing samples were measured in tapping mode in air at room temperature and were conducted using SiN-type cantilevers (DNP-10, 0.35 N m^{-1}, Bruker) [29]. The images of all samples were acquired over areas of 500 × 500 nm.

2.7. Dynamic light scattering measurements

The instrument Dynapro Titan TC (Wyatt Technology, US) was used on the light scattering DLS measurements for single and mixed foulants size determination and aggregation degree. The solutions were placed in the sample chamber that was temperature regulated for measurements at 25℃. Samples were filtrated by 0.45-μm filter membrane.

3. Results and discussion

3.1. Effect of pH on single fouling system

The effect of pH on membrane fouling was investigated using single HA, BSA, or LYS system, while keeping the total feed organic foulant concentration at 20 mg L^{-1}. Fig. 1(a) shows that the effect of pH value on HA membrane fouling behavior was not significant, and the permeate flux did not vary until 15 h of the experiment. The most fouling behavior occurred at pH 4.5, and the decline ratio of permeate flux was approximately 10.0% over 30 h. However, the flux declines at other pH values were not obvious and less than 4.9% decline, which may be attributed to the mass reduction of HA deposited on NF membrane with increasing of pH [14]. Fig. 1(b) and (c) show the effect of pH on macromolecule (BSA and LYS) fouling behavior on the membrane, respectively. The permeate flux of the NF membrane fouled by single BSA system decreased by 11.2, 8.4, 5.4, and 4.5%, and that of single LYS system decreased by 10.7, 15.3, 15.4, and 8.6%, respectively, within the range of pH 4.5–10.5 over 30 h. The most severe fouling behaviors by BSA or LYS proteins alone occurred at pH 4.5 or 8.5,

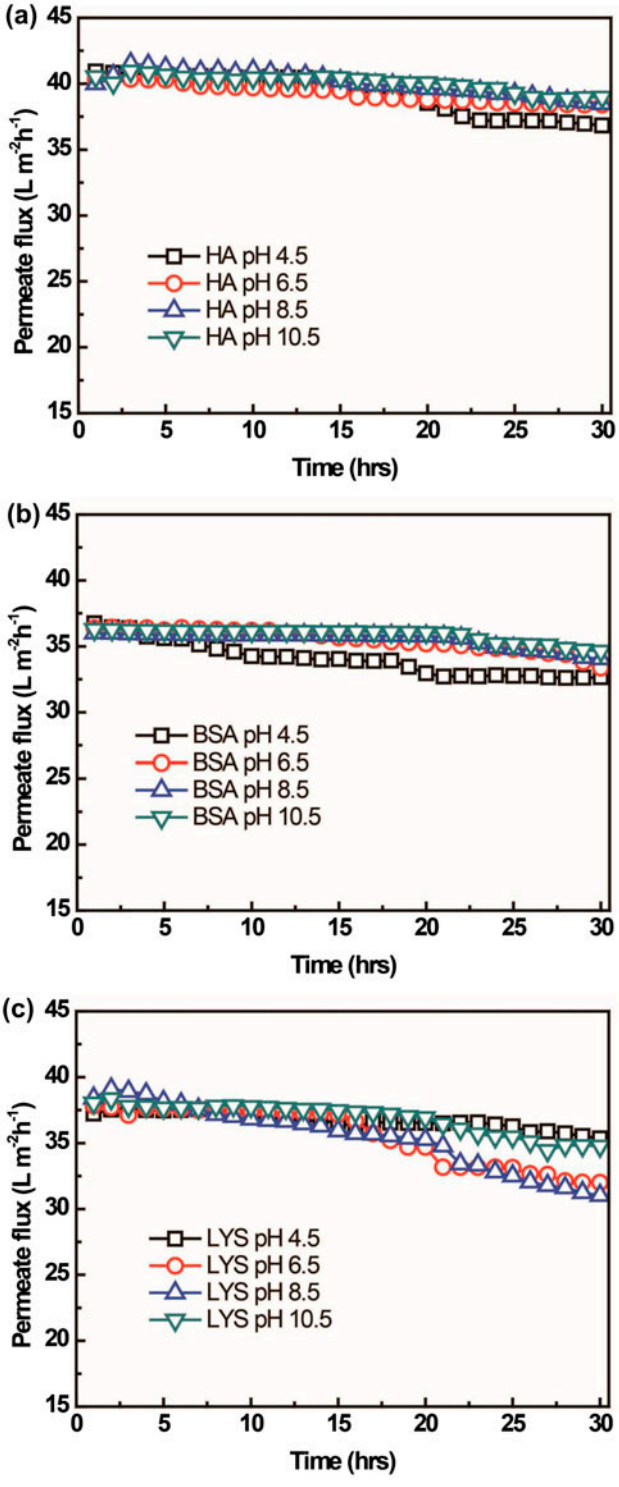

Fig. 1. Effect of solution pH on single system (HA, BSA, or LYS) in the presence of inorganic salt and total pollutant concentration of 20 mg L^{-1}. (a) HA-fouled, (b) BSA-fouled, and (c) LYS-fouled behavior. Test conditions: ionic strength of 10 mM at 25˚C.

respectively, moreover the pH values were closed to isoelectric points of the corresponding BSA and LYS [15,21].

3.2. Effect of pH on mixed fouling system

The effect of pH on membrane fouling by BSA + HA and LYS + HA mixed systems was investigated, while keeping the total foulant concentration at 20 mg L^{-1} and the concentration ratio of BSA (LYS): HA at 1:1 w/w. Fig. 2(a) and (b) demonstrate the effect of pH on BSA + HA and LYS + HA mixture fouling within pH range of 4.5–10.5. Fig. 2(a) shows

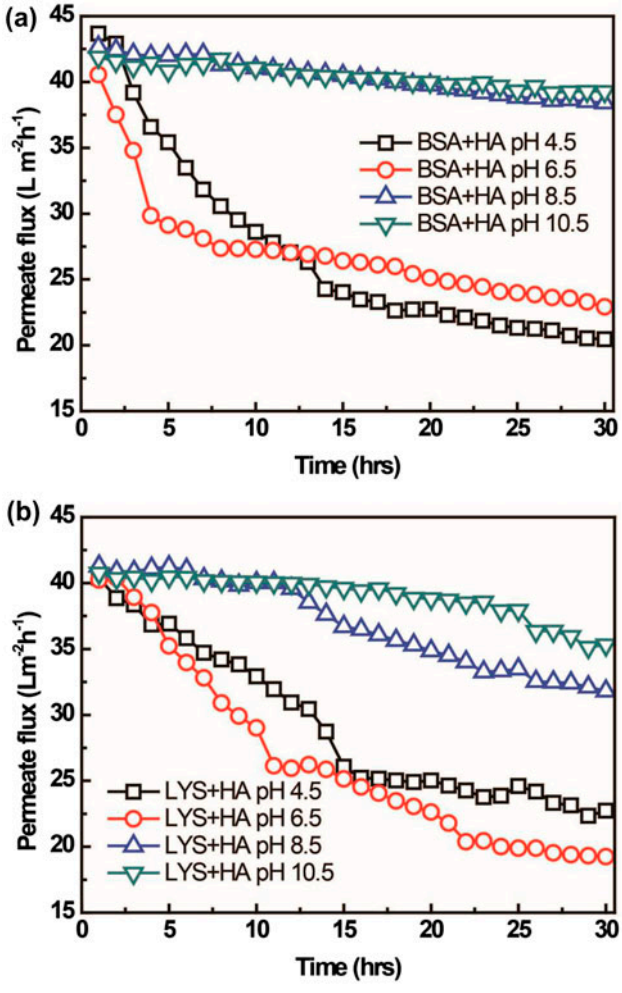

Fig. 2. Effect of solution pH on mixed system in the presence of inorganic salt and total pollutant concentration of 20 mg L^{-1}. (a) BSA + HA fouling system and (b) LYS-HA fouling system. Test conditions: ionic strength of 10 mM at 25˚C.

that the permeate flux at pH 4.5 and 6.5 evidently declined at the first stage. The fouling behavior of BSA + HA at pH 4.5 was the severest among the fouling behavior at other pH values, and the flux declined by 53.2% over 30 h. The flux also declined by 43.5% at pH 6.5. However, the fouling behaviors of BSA + HA at pH 8.5 and 10.5 were the slight, with the flux rate declined to only 11.1 and 6.3%, respectively. Similar phenomenon was observed in the fouling behavior of LYS + HA mixture on the NF membrane, wherein permeate flux loss occurred at the initial stage under acidic condition. However, the severest fouling of LYS + HA occurred at pH 6.5, and the flux declined by 52.4% over 30 h of fouling test in Fig. 2(b). The permeate flux of LYS + HA declined by 43.8% at pH 4.5, by contrast, flux losses at pH 8.5 and 10.5 were less and only 20.4 and 13.8%, respectively. The macromolecular polymers formed by BSA/LYS and organic acid were easily absorbed on the membrane; hence, the permeate flux declined obviously at acidic and neutral conditions [17,20].

3.3. AFM characterization of virgin and fouled NF membrane

Membrane surface roughness was measured based on AFM images of virgin and the most severe fouling membranes by single foulant alone, as shown in Table 1 and Fig. 3. The virgin DL membrane revealed a relatively smooth and homogenous surface structure, with R_a of 13.4 nm and R_q of 16.2 nm according to Fig. 3(a). As the fouling behavior of NF membrane by HA, BSA, or LYS alone was slight, the severest fouled membranes by HA at pH 4.5, BSA at pH 4.5, and LYS pH 8.5 were measured, respectively. The R_a value of the membrane fouled by HA, BSA, or LYS is 17.2, 17.9, or 21.5 nm, respectively, and R_q of the membrane fouled by HA, BSA, or LYS was 21.2, 22.1, or 26.5 nm, respectively. Combination of the above permeate flux declines discussion, the rougher surface indicates the more severe fouling behavior.

Figs. 4 and 5 show the AFM images of the membrane fouled by mixed foulant BSA + HA and

Table 1
Surface roughness parameters of virgin and fouled membrane by single foulant

	Virgin membrane	HA fouled (pH 4.5)	BSA fouled (pH 4.5)	LYS fouled (pH 8.5)
R_a (nm)	13.4	17.2	17.9	21.5
R_q (nm)	16.2	21.2	22.1	26.5

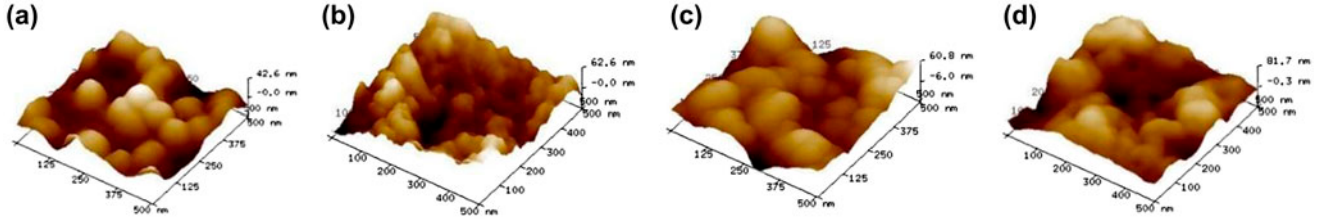

Fig. 3. AFM images of (a) virgin membrane, (b) HA-fouled membrane at pH 4.5, (c) BSA-fouled membrane at pH 4.5, and (d) LYS-fouled membrane at pH 8.5.

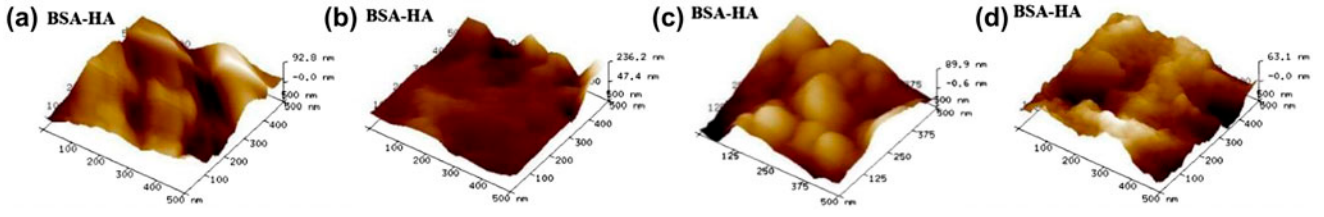

Fig. 4. AFM images of BSA + HA-fouled membrane at pH (a) 4.5, (b) 6.5, (c) 8.5, and (d) 10.5.

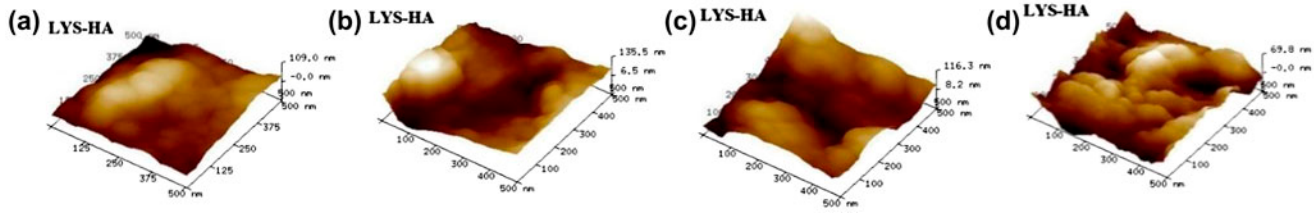

Fig. 5. AFM images of LYS + HA-fouled membrane at pH (a) 4.5, (b) 6.5, (c) 8.5, and (d) 10.5.

Table 2
Comparison of fouled NF membrane surface roughness by BSA + HA and LYS + HA at variant pH

	BSA + HA (pH)				LYS + HA (pH)			
	4.5	6.5	8.5	10.5	4.5	6.5	‘8.5	10.5
R_a (nm)	25.9	24.8	17.9	17.0	27.5	29.5	21.5	20.5
R_q (nm)	31.4	37.4	22.1	21.5	34.8	34.4	26.5	25.3

LYS + HA, wherein the R_a and R_q values of BSA + HA-fouled, or of LYS + HA-fouled membrane at variant pH are depicted in Table 2. For BSA + HA system, R_a values increased from 17.0 to 25.9 nm with solution pH lower. Similarly, R_a values enhanced with decreasing of pH at LYS + HA system. However, the most R_a values occurring at pH 6.5 was 29.5 nm. The increased roughness of the fouled membrane was due to the accumulation of mixed organic aggregates on the membrane surface [30–32].

3.4. Zeta potential of single/mixed system

The interaction of single or mixed fouling system transformation at different zeta potential values was investigated. Fig. 6 shows that zeta potential values of single (HA, BSA, and LYS) and mixed systems (BSA + HA and LYS + HA) were presented at a pH range of 4.0–11.0. Fig. 6(a) shows that the zeta potential of HA was negative from –23.6 ± 1.6 mV to –37.4 ± 2.7 mV at a pH range of 4.1–10.9. Furthermore, the zeta potential values of BSA and LYS decreased as increasing solution pH. The IEP of BSA and LYS was at pH 4.7 and 10.1, respectively, according to the values measured by zeta potential equipment and reported in the literature [27,33]. As Fig. 6(b) illustrated, the IEPs of BSA + HA and LYS + HA mixed matters migrated to acid when the protein solution mixed with the equal mass concentration of HA in the solution. The IEP of BSA + HA mixed system appeared at < ~pH 4.0 comparing with 4.7 of BSA, whereas the IEP of LYS + HA mixed system migrated further and appeared at ~pH 6.5 comparing with 10.1 of LYS. The zeta potential of BSA + HA declined from –4.8 ± 2.3 mV to –40.1 ± 0.6 mV, and that of LYS + HA also declines from 15.4 ± 0.4 mV to –21.5 ± 0.1 mV with enhancing the solution pH. This results were attributed to the composition of BSA-HA/(LYS-HA) aggregations by hydrophobic groups, hydrogen bond, or electrostatic interaction [34].

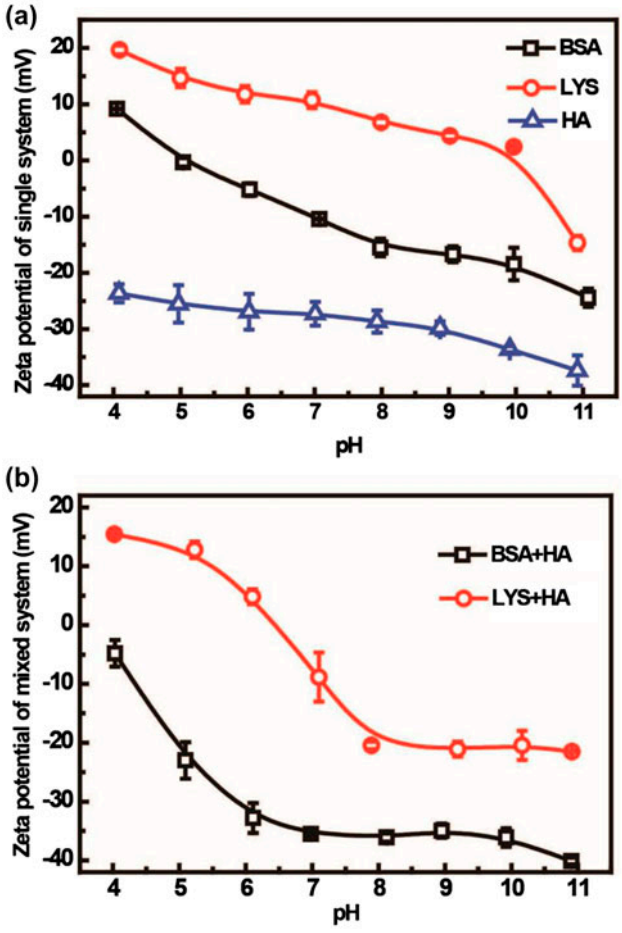

Fig. 6. Zeta potential of single and mixed systems as a function of pH. (a) Single system: HA, BSA, and LYS; and (b) mixed system: BSA + HA and LYS + HA. Similar mass concentration was maintained for both single and mixed systems. At least two replicates were performed for each pH value.

Table 3
Permeate flux decline and zeta potential of single and mixed systems as a function of pH. Single system: HA, BSA, and LYS; and mixed system: BSA + HA and LYS + HA. Similar mass concentration was maintained for both single and mixed systems. At least two replicates were performed for each pH value

	pH 4.5		pH 6.5		pH 8.5		pH 10.5	
	Zeta potential (mV)	Permeate flux decline (%)	Zeta potential (mV)	Permeate flux decline (%)	Zeta potential (mV)	Permeate flux decline (%)	Zeta potential (mV)	Permeate flux decline (%)
HA	–24.7	9.7	–27.0	4.5	–29.3	4.3	–35.8	3.9
BSA	4.2	11.2	–7.5	7.8	–16.4	5.0	–21.1	4.5
LYS	17.2	8.0	11.1	13.8	5.1	17.3	–5.7	8.6
BSA + HA	–13.5	52.0	–34.1	42.1	–35.4	10.5	–38	5.8
LYS + HA	15.0	42.4	0.1	52.1	–20.2	20.9	–20.7	12.3

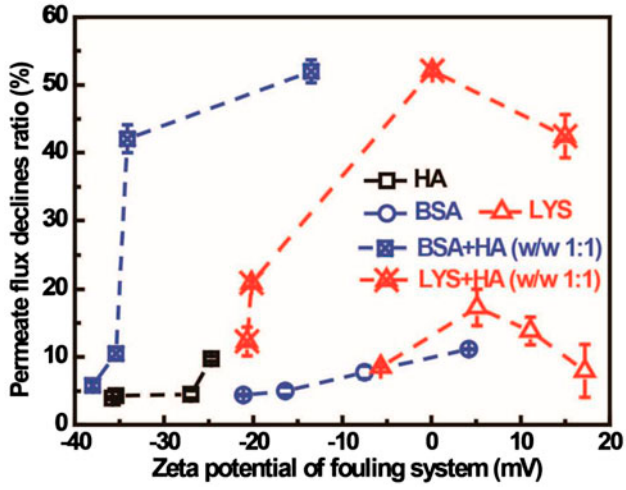

Fig. 7. Effect of zeta potential of single/mixed systems on permeate flux declines.

3.5. Comparison of zeta potential on single/mixed fouling system

Table 3 depicts the permeate flux decline ratio of single and mixed foulant systems at different zeta potential values over 30 h of filtration, wherein the mass concentration of solute and hydraulic conditions was the same. Fig. 7 illustrates that the fouling degree of single HA system aggravated with zeta potential value of HA lower. Relatively, the most severe fouling by BSA and LYS system occurred at 4.2 and 5.1 mV, respectively, closed to zero potential. This result was attributed to the more organic molecules deposited on the membrane with lower zeta potential value, thereby forming thicker and tighter "cake" on the membrane [22,27]. However, when zeta potentials of BSA and LYS were –7.5 and –5.7 mV, respectively, near zero potential, the permeate flux declines of both BSA and LYS system were about two thirds of declines by corresponding positive charge. Which was attributed that BSA or LYS aggregates with positive charge adsorbed more easily on the membrane surface by electrostatic attraction, considering that polyamide effective rejection layer of NF membrane was negative charge. Comparing two single protein fouling systems, the results indicated that the permeate flux loss at 30 h was just 5.0%, when the zeta potential of BSA was ≥–16.4 mV, similarly, when the zeta potential of the LYS was ≥17.2 mV, the permeate flux loss at 30 h was only 8.0%. For single fouling system, the electrostatic force between the molecules held a dominant position, wherein the lower zeta potential value of the single system means the more severe permeate flux. For BSA + HA mixed foulants, the most decreasing of flux achieved 52.0% and occurred at zeta potential of –13.5 mV. Within the zeta potential range of –13.5 to –34.5 mV, BSA-HA polymer aggregated by

Table 4
Size distribution of single protein foulants at variant pH

	BSA (pH)				LYS (pH)			
	4.5	6.5	8.5	10.5	4.5	6.5	8.5	10.5
Mean diameter (nm)	8.4	7.3	6.9	5.3	5.5	5.8	7.2	5.9
%Pd	33.3	17.2	29.1	52.9	17.6	62.7	37.4	37.6

Table 5
Size distribution of mixed foulants at variant pH

	BSA + HA (pH)				LYS + HA (pH)			
	4.5	6.5	8.5	10.5	4.5	6.5	8.5	10.5
Mean diameter (nm)	12.1	12.8	7.3	6.9	9.8	9.6	8.5	5.5
%Pd	84.0	18.3	59.0	44.8	25.0	16.6	11.5	44.8

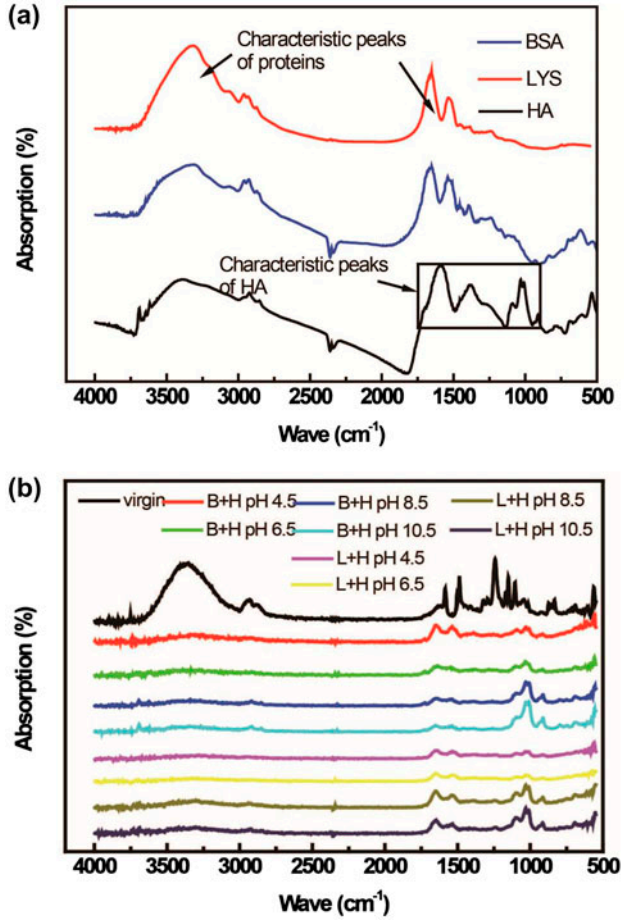

Fig. 8. ATR-FT-IR spectra of (a) single foulants and (b) virgin and fouled membranes by mixed system (BSA + HA and LYS + HA) at different pH values.

hydrogen bond or hydrophobic group was present, and aggravates fouling on the NF membrane. Thus, the decline in permeate flux by BSA + HA was over 40% at 30 h. With the increased pH value above 8.5, the zeta potential of BSA + HA was superior at –35.4 mV. The fouling degree alleviated to 8.5%. Similar fouling behavior occurred at LYS + HA mixed system within zeta potential of 15.0 to –20.7 mV. As Fig. 7 shown, the zeta potential value of LYS-HA at pH 6.5 was the lowest and only 0.1 mV, indicating that more LYS-HA polymers formed by hydrogen bond or hydrophobic group can be absorbed on the membrane surface. This phenomenon was the severest fouling with permeate flux loss of over 50%. The zeta potential value of LYS-HA was 15.0 and –20.2 mV at pH 4.5 and 8.5, respectively. However, permeate flux loss at 15.0 mV was twice than that at –20.2 mV. This result indicated that positively charged LYS-HA aggregate can absorb more easily on the membrane than negatively charged one. With the pH value increased to 10.5, stronger electrostatic repulsive force between the LYS-HA aggregate monomers can hinder further polymer formation.

As for the effect of the fouling cake layers on the membrane fouling behavior, the polymers aggregated, and membranes fouled by both single and mixed foulants at variant pH values were presented by the DLS and ATR-FT-IR, respectively. Tables 4 and 5 show the intensity size distribution and aggregation for both single protein and mixed foulants measured at different pH. For single BSA system, within pH 4.5–10.5, the size distributions were 8.4–5.3 nm, respectively. Moreover, the size distribution of mono BSA molecule was about 3.6 nm. The results suggested that the feed contained multi-aggregates of two and three BSA particles below pH 8.5; reversely, the main existence in the feed was BSA monomer at pH 10.5. For single LYS system, within pH 4.5–10.5, the major peak in the size distribution was 5.5–7.2 nm, respectively. Moreover, the size distribution of mono LYS molecule was about 1.9 nm. Comparing with BSA system, the results illustrated that LYS molecules can connect covalently, and form polymer easily by disulfide bond between LYS. While BSA (LYS) combined with HA, aggregation of BSA-HA/LYS-HA can increase 1–2 times than that of BSA or LYS alone within the range of pH 4.5–10.5. As the molecular size of HA was the range of 0.3–0.9 nm, onefold formation, which proteins wrapped with HA, can hardly form the aggregation according to Table 5. Therefore, the results indicated that HA can be attributed to bridging between macro-molecules, e.g. BSA or LYS.

As shown in Fig. 8(a), the characteristic peaks of BSA and LYA proteins were at the wavelength of

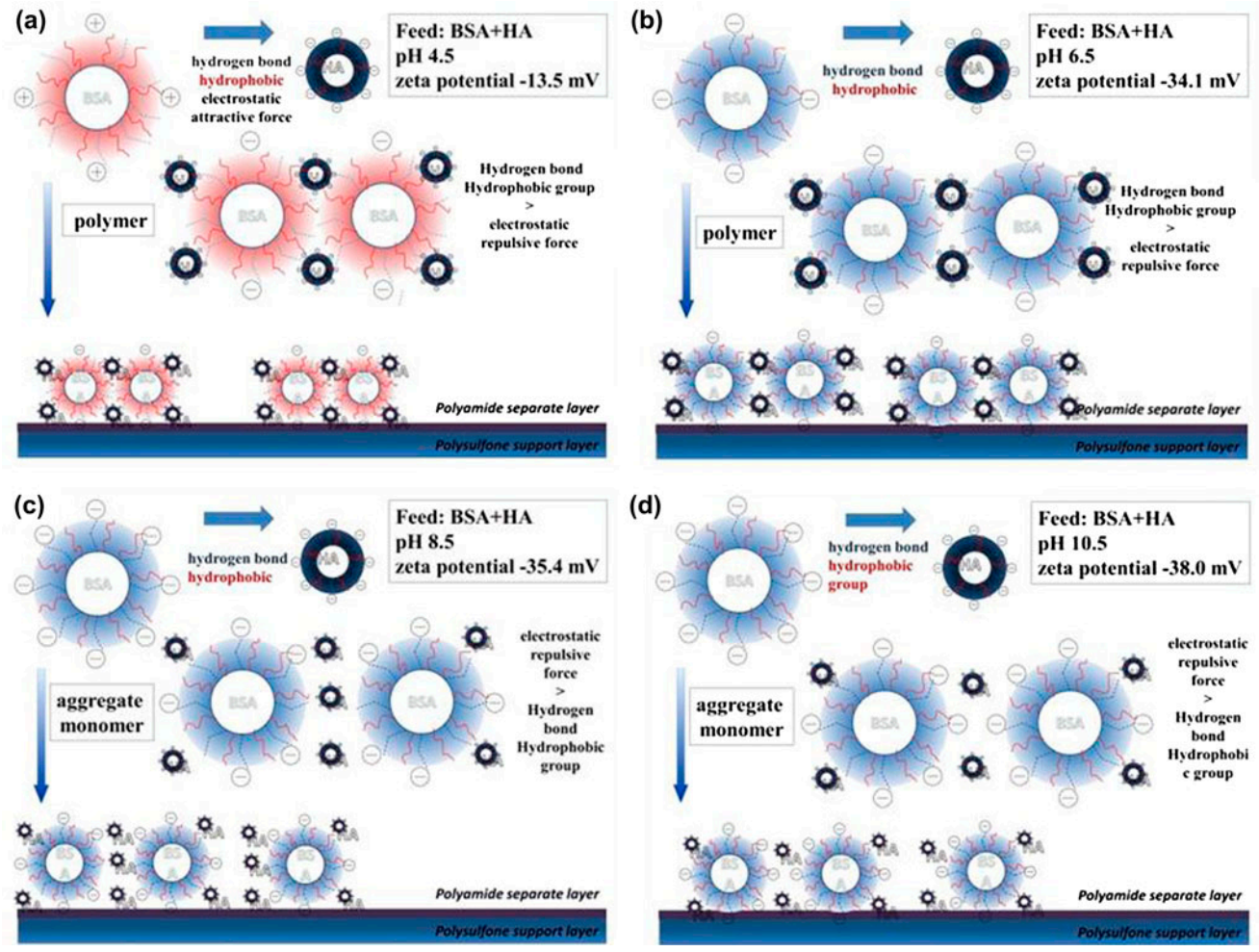

Fig. 9. Description of aggregate formation and fouling behavior of BSA + HA at pH (a) 4.5, (b) 6.5, (c) 8.5, and (d) 10.5.

3,313, 2,960, 2,928, 1,653, and 1,537 cm^{-1}. The peaks identifying HA organic acid at the wavelengths of 1,570, 1,377, and 1,032 cm^{-1} and the weak peak at 3,400–3,000 cm^{-1} represented the phenolic or alcohol hydroxyl groups. The broad peak at the wavelength of 3,360 cm^{-1} was a complex one because of the overlapping of N–H stretching and carboxylic groups of the polyamide layer, whereas the relative weak peaks at 2,945 and 2,887 cm^{-1} can be assigned to the C–H stretching vibration of aliphatic chain [8]. As shown in Fig. 8(b), with the spectra in the range of 1,600–800 cm^{-1}, a relatively weak peak observed at the wavelength of 873 or 833 cm^{-1} corresponded to 1,4-disubstituted benzene. In addition, the spectra exhibited evident absorbance at 1,584, 1,503, and 1,487 cm^{-1}, which were the characteristic for polysulfone [35]. The DL membrane had higher intensity for some peaks; for example, at wavelengths of 1,242, 1151.5, and 1,105 cm^{-1}, most peaks corresponded to the hydrophilic functional groups of polyamide layer. After 30 h of filtration by mixed foulants at different pH values, the fouled NF membranes show that several diagnostic peaks disappeared, and some novel peaks that identified the potential foulants could be found. For instance, the broad peak N–H stretching and carboxylic groups at the wavelength of 3,358 cm^{-1} disappeared when the pH value was lower than 6.5 at BSA + HA mixed system. Moreover, novel peaks identifying BSA protein and HA organic acid were observed at the wavelengths of 1,653 and 1,533 cm^{-1} and 1,033 and 912 cm^{-1}, respectively. However, the peak identifying the protein functional groups at the wavelength of 3,313 cm^{-1} was yet to be discovered, because the main foulant forming the "cake" on the membrane was -$[BSA\text{-}HA]_n$- polymer. However, when the pH value of BSA + HA mixed system was superior

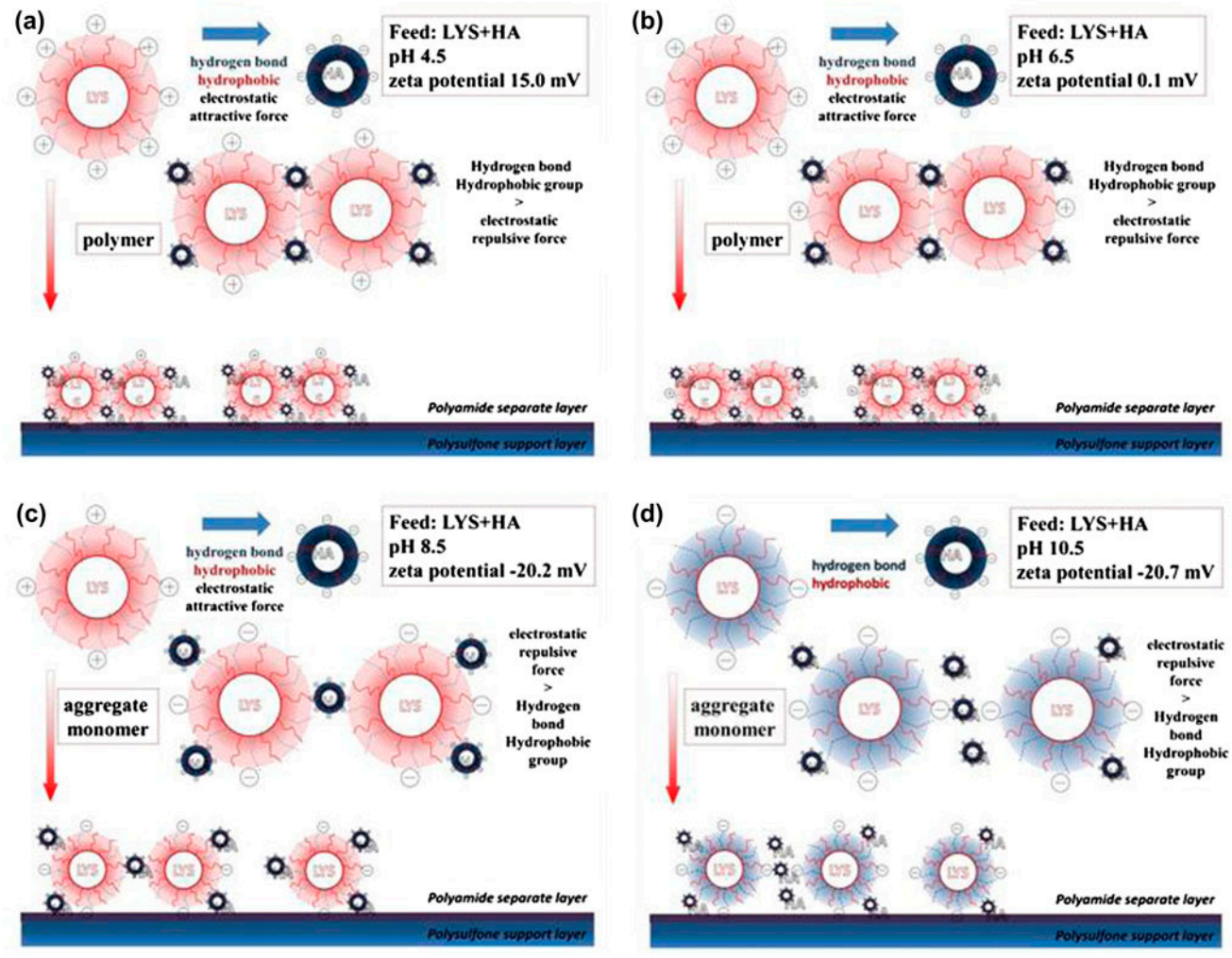

Fig. 10. Description of aggregate formation and fouling behavior of LYS + HA at pH (a) 4.5, (b) 6.5, (c) 8.5, and (d) 10.5.

at 8.5, stronger peaks appeared at 1,093, 1,033, and 912 cm^{-1}. This result demonstrated that the dominantly formed foulant absorbed on the membrane was HA, and HA-BSA-HA aggregate monomers in the feed solution, according to the identified functional groups on the membrane. Similar results were presented by the characteristic of NF membrane fouled by LYS + HA mixed systems at variant pH values, as shown in Fig. 8(b), which depicted the formation of -[LYS-HA]$_n$- polymer at the LYS + HA system with a pH ranging from 4.5 to 6.5. With the pH value shifted to 8.5, the main fouling formation converted -[LYS-HA]$_n$- polymer into HA-LYS-HA aggregate monomers. At pH 10.5, the main foulants formed and absorbed on the membrane were HA-LYS-HA aggregate monomers or LYS-LYS (HA-HA).

3.6. Proposed mixed fouling mechanism and foulant structure

Using the model organic foulants, solution pH was a significant factor on the NF membrane fouling behavior because of its effect on the aggregate composition of protein and organic acid. Moreover, the model fouling systems and fouling membrane at variant pH were verified by Zetasize Nano-ZS, DLS, AFM, and ATR-FT-IR analyses, respectively. The fouling mechanisms of BSA (LYS) and HA mixed foulants at variant pH values were depicted in Figs. 9 and 10.

During the fouling in BSA + HA system, the organic macromolecules tended to be a curl of clusters by the interaction of hydrophobic functional group and hydrogen bond between BSA and HA [36]. Therefore, more molecular weight and complex space

dimension of -[BSA-HA]$_n$- polymer aggregated at low pH (≤~6.5), following the absorbance of polymer on the membrane, changing the hydrophilicity and roughness of the membrane surface, and finally fouling cake formation led to permeate flux decline. In particular, when the solution pH value was about 4.5, the electrostatic attractive force between BSA and HA contributed to the bridged interaction and formation of tighter polymer in the solution [37]. This result led to severest flux decline. At pH 6.5, the molecular interaction between BSA and HA mainly existed in the solution; however, electrostatic repulsion between BSA and HA may weaken this interaction. Thus, the density of polymer at pH 6.5 was looser than that at pH 4.5. With pH value enhanced to above 8.5, the electrostatic repulsion between BSA and HA may further enhance and become dominant. Therefore, HA molecules may no longer function as the bridge between proteins. On the contrary, a part of HA molecules was absorbed on the BSA macromolecules. Furthermore, an amount of free HA molecules at the ambient BSA macromolecules formed a similar barrier layer through the strong electrostatic repulsive force between BSA and HA. The polymerized monomers of HA-BSA-HA with strong negative charge were stable that the monomers could not aggregate polymer -[BSA-HA]$_n$- in the solution, according to extended DLVO theory [38,39]. Moreover, the electrostatic repulsion between monomer and membrane surface decreased the adhesion of organic foulant on the membrane.

For LYS + HA system, HA molecules can also primarily bridge LYS molecules through the interaction of hydrophobic group and hydrogen bond. Moreover, larger molecular and more complex space dimension of -[LYS-HA]$_n$- polymers including a hydration layer can provide energy during absorption at low pH (≤~8.5), following the increased amount of polymer absorbed on the membrane and finally, fouling cake formation leading to permeate flux decline [40]. In particular, when the solution pH was approximately 6.5, the zeta potential value of -[LYS-HA]$_n$- polymer was about 0.1 mV, and the electrostatic force among the polymers was the weakest. Thus, polymers with compact structure in the solution led to rapid foulant deposition and resulted in severest flux decline [24,41]. Both monomer and polymer of LYS-HA in the feed were presented at pH 4.5 and 8.5, when their zeta potential values are 15.0 and −20.2 mV, respectively. Electrostatic repulsion in -[LYS-HA]$_n$- polymer may weaken the compactness of the polymer structure. Thus, the density of foulant on the membrane at pH 4.5 or 8.5 was looser than that at pH 6.5. With the pH value enhanced to 10.5, the electrostatic repulsion between LYS and HA may further enhance and become major factor. Therefore, HA molecules may no longer function as the bridge between macro-molecule proteins. On the contrary, HA molecules form a similar barrier layer at the ambient LYS molecules by the strong electrostatic repulsion. Furthermore, the formation of polymerized monomer HA-LYS-HA with strong negative charge was stable that the monomers could not aggregate -[LYS-HA]$_n$- polymer in the solution. The electrostatic repulsion between monomer and membrane surface also decreased the adhesion of organic foulant on the membrane.

4. Conclusion

This study investigated the characteristics of single/mixed organic foulants on NF membrane and the effect of solution pH on single or mixed fouling system.

(1) The fouling behavior of the mixed system was severer than that of the single system under the same experimental conditions. When the pH was above 6.5, the organic fouling degree decreased with increasing solution pH.
(2) The most dramatic fouling in single and mixed systems appeared near the IEPs (single system: HA, BSA, and LYS at −24.7, 4.2, and 5.1 mV, respectively; and mixed system: BSA + HA and LYS + HA at −13.5 and 0.1 mV, respectively). When BSA (or LYS) and HA exhibited opposite charges, the electrostatic attractive force between BSA (or LYS) and HA can form BSA (LYS)-HA aggregate monomers. Moreover, the zeta potential value of aggregate monomers was low, the hydrogen bond and hydrophobic interactions of BSA-/LYS-HA were dominant, and protein and organic acid were polymer -[BSA-/LYS-HA]$_n$-. When BSA (or LYS) and HA had weaker-like charges, the hydrogen bond and hydrophobic group between BSA (or LYS) and HA can take over and form polymer -[BSA-/LYS-HA]$_n$-, which mainly existed along with BSA-/LYS-HA in the feed. When BSA (or LYS) and HA had higher-like charges, the stronger electrostatic repulsive force between BSA (or LYS) and HA can hinder the formation of BSA (LYS)-HA aggregate monomers, and BSA (LYS)-HA, BSA (LYS)-BSA (LYS), and HA-HA were mainly formed.
(3) When analyzing the zeta potential value and composition of foulants in the feed with a complex system, zeta potential can be considered as the predictor of fouling behavior, and the basis to clean the NF membrane.

References

[1] F. Beyer, B.M. Rietman, A. Zwijnenburg, P.v.D. Brink, J.S. Vrouwenvelder, M. Jarzembowska, J. Laurinonyte, A.J.M. Stams, C.M. Plugge, Long-term performance and fouling analysis of full-scale direct nanofiltration (NF) installations treating anoxic groundwater, J. Membr. Sci. 468 (2014) 339–348.

[2] A. Pérez-González, R. Ibáñez, P. Gómez, A.M. Urtiaga, I. Ortiz, J.A. Irabien, Nanofiltration separation of polyvalent and monovalent anions in desalination brines, J. Membr. Sci. 473 (2015) 16–27.

[3] R. Hepsen, Y. Kaya, Optimization of membrane fouling using experimental design: An example from dairy wastewater treatment, Ind. Eng. Chem. Res. 51 (2012) 16074–16084.

[4] A. Somrani, A.H. Hamzaoui, M. Pontie, Study on lithium separation from salt lake brines by nanofiltration (NF) and low pressure reverse osmosis (LPRO), Desalination 317 (2013) 184–192.

[5] N. Askari, M. Farhadian, A. Razmjou, H. Hashtroodi, Nanofiltration performance in the removal of dye from binary mixtures containing anthraquinone dyes, Desalin. Water Treat. (2015) 1–8, doi: 10.1080/19443994.2015.1090917.

[6] R. Ma, Y. Xie, S. Xia, B. Xu, B. Dong, N. Gao, Ametryn removal with nanofiltration membranes, Desalin. Water Treat. 29 (2011) 331–335.

[7] A.H.M.A. Sadmani, R.C. Andrews, D.M. Bagley, Impact of natural water colloids and cations on the rejection of pharmaceutically active and endocrine disrupting compounds by nanofiltration, J. Membr. Sci. 450 (2014) 272–281.

[8] J. Fang, B. Deng, Rejection and modeling of arsenate by nanofiltration: Contributions of convection, diffusion and electromigration to arsenic transport, J. Membr. Sci. 453 (2014) 42–51.

[9] A. Simon, W.E. Price, L.D. Nghiem, Changes in surface properties and separation efficiency of a nanofiltration membrane after repeated fouling and chemical cleaning cycles, Sep. Purif. Technol. 113 (2013) 42–50.

[10] N. Her, G. Amy, H.-R. Park, M. Song, Characterizing algogenic organic matter (AOM) and evaluating associated NF membrane fouling, Water Res. 38 (2004) 1427–1438.

[11] H. Seungkwan, E. Menachem, Chemical and physical aspects of natural organic matter (NOM) fouling of nanofiltration membranes, J. Membr. Sci. 132 (1997) 159–181.

[12] Y. Song, T. Li, J. Zhou, F. Pan, B. Su, C. Gao, Comprehensive pilot-scale investigation of seawater nanofiltration softening by increasing permeate recovery with recirculation, Desalin. Water Treat. (2015) 1–12, doi: 10.1080/19443994.2015.1084531.

[13] L.D. Nghiem, D. Vogel, S. Khan, Characterising humic acid fouling of nanofiltration membranes using bisphenol A as a molecular indicator, Water Res. 42 (2008) 4049–4058.

[14] C.Y. Tang, Y.-N. Kwon, J.O. Leckie, Fouling of reverse osmosis and nanofiltration membranes by humic acid—Effects of solution composition and hydrodynamic conditions, J. Membr. Sci. 290 (2007) 86–94.

[15] H. Mo, K.G. Tay, H.Y. Ng, Fouling of reverse osmosis membrane by protein (BSA): Effects of pH, calcium, magnesium, ionic strength and temperature, J. Membr. Sci. 315 (2008) 28–35.

[16] A.E. Contreras, A. Kim, Q. Li, Combined fouling of nanofiltration membranes: Mechanisms and effect of organic matter, J. Membr. Sci. 327 (2009) 87–95.

[17] D.T. Myat, M.B. Stewart, M. Mergen, O. Zhao, J.D. Orbell, S. Gray, Experimental and computational investigations of the interactions between model organic compounds and subsequent membrane fouling, Water Res. 48 (2014) 108–118.

[18] M.R. Teixeira, V.S. Sousa, Fouling of nanofiltration membrane: Effects of NOM molecular weight and microcystins, Desalination 315 (2013) 149–155.

[19] Y. Xie, C. Guo, R. Ma, B. Xu, N. Gao, B. Dong, S. Xia, Effect of dissolved organic matter on arsenic removal by nanofiltration, Desalin. Water Treat. 51 (2013) 2269–2274.

[20] R. Chan, V. Chen, The effects of electrolyte concentration and pH on protein aggregation and deposition: Critical flux and constant flux membrane filtration, J. Membr. Sci. 185 (2001) 177–192.

[21] Y.-N. Wang, C.Y. Tang, Protein fouling of nanofiltration, reverse osmosis, and ultrafiltration membranes—The role of hydrodynamic conditions, solution chemistry, and membrane properties, J. Membr. Sci. 376 (2011) 275–282.

[22] K.L. Jones, C.R. O'Melia, Protein and humic acid adsorption onto hydrophilic membrane surfaces: Effects of pH and ionic strength, J. Membr. Sci. 165 (2000) 31–46.

[23] Q. She, C.Y. Tang, Y.-N. Wang, Z. Zhang, The role of hydrodynamic conditions and solution chemistry on protein fouling during ultrafiltration, Desalination 249 (2009) 1079–1087.

[24] L. Palacio, C.C. Ho, P. Prádanos, A. Hernández, A.L. Zydney, Fouling with protein mixtures in microfiltration: BSA–lysozyme and BSA–pepsin, J. Membr. Sci. 222 (2003) 41–51.

[25] A.W. Seng, E. Menachem, Protein (BSA) fouling of reverse osmosis membranes: Implications for wastewater reclamation, J. Membrane Sci. 296 (2007) 83–92.

[26] F. Xiao, P. Xiao, W.J. Zhang, D.S. Wang, Identification of key factors affecting the organic fouling on low-pressure ultrafiltration membranes, J. Membr. Sci. 447 (2013) 144–152.

[27] Y.-N. Wang, C.Y. Tang, Fouling of nanofiltration, reverse osmosis, and ultrafiltration membranes by protein mixtures: The role of inter-foulant-species interaction, Environ. Sci. Technol. 45 (2011) 6373–6379.

[28] Y.-N. Wang, C.Y. Tang, Nanofiltration membrane fouling by oppositely charged macromolecules: Investigation on flux behavior, foulant mass deposition, and solute rejection, Environ. Sci. Technol. 45 (2011) 8941–8947.

[29] D.J. Johnson, S.A.A. Malek, B.A.M. Al-Rashdi, N. Hilal, Atomic force microscopy of nanofiltration membranes: Effect of imaging mode and environment, J. Membr. Sci. 389 (2012) 486–498.

[30] Y. Ye, P.L. Clech, V. Chen, A.G. Fane, B. Jefferson, Fouling mechanisms of alginate solutions as model extracellular polymeric substances, Desalination 175 (2005) 7–20.

[31] D. Nanda, K.-L. Tung, Y.-L. Li, N.-J. Lin, C.-J. Chuang, Effect of pH on membrane morphology, fouling potential, and filtration performance of nanofiltration membrane for water softening, J. Membr. Sci. 349 (2010) 411–420.
[32] L. Wang, R. Miao, X. Wang, Y. Lv, X. Meng, Y. Yang, D. Huang, L. Feng, Z. Liu, K. Ju, Fouling behavior of typical organic foulants in polyvinylidene fluoride ultrafiltration membranes: Characterization from microforces, Environ. Sci. Technol. 47 (2013) 3708–3714.
[33] S.P. Palecek, A.L. Zydney, Intermolecular electrostatic interactions and their effect on flux and protein deposition during protein filtration, Biotechnol. Progr. 10 (1994) 207–213.
[34] D. Jermann, W. Pronk, S. Meylan, M. Boller, Interplay of different NOM fouling mechanisms during ultrafiltration for drinking water production, Water Res. 41 (2007) 1713–1722.
[35] S. Belfer, R. Fainchtain, Y. Purinson, O. Kedem, Surface characterization by FT-IR-ATR spectroscopy of polyethersulfone membranes-unmodified, modified and protein fouled, J. Membr. Sci. 172 (2000) 113–124.
[36] C.Y. Tang, Y.-N. Kwon, J.O. Leckie, Characterization of humic acid fouled reverse osmosis and nanofiltration membranes by transmission electron microscopy and streaming potential measurements, Environ. Sci. Technol. 41 (2007) 942–949.
[37] P. Xiao, F. Xiao, W. Zhang, B. Zhao, D. Wang, Insight into the combined colloidal-humic acid fouling on the hybrid coagulation microfiltration membrane process: The importance of aluminum, Colloids Surf., A 461 (2014) 98–104.
[38] J.A. Brant, A.E. Childress, Assessing short-range membrane–colloid interactions using surface energetics, J. Membr. Sci. 203 (2002) 257–273.
[39] E.M.V. Hoek, G.K. Agarwal, Extended DLVO interactions between spherical particles and rough surfaces, J. Colloid Interface Sci. 298 (2006) 50–58.
[40] H. Zhang, L.-M. Hu, C.-G. Lin, L. Wang, S.-L. Yuan, Molecular dynamics simulation of interaction between lysozyme and non-fouling polymer membranes, Acta Polym. Sin. 21 (2014) 99–106.
[41] C. Güell, R.H. Davis, Membrane fouling during microfiltration of protein mixtures, J. Membr. Sci. 119 (1996) 269–284.